Stem Cell Reports
Report
ISSCR
OPEN ACCESS

Effects of Spaceflight on Human Induced Pluripotent Stem Cell-Derived Cardiomyocyte Structure and Function

Alexa Wnorowski,[1,2,11] Arun Sharma,[1,3,4,5,11] Haodong Chen,[1,3] Haodi Wu,[1,3] Ning-Yi Shao,[1,3] Nazish Sayed,[1,3] Chun Liu,[1,3] Stefanie Countryman,[6] Louis S. Stodieck,[6] Kathleen H. Rubins,[7] Sean M. Wu,[1,3,8] Peter H.U. Lee,[9,10] and Joseph C. Wu[1,3,8,*]

[1]Stanford Cardiovascular Institute, Stanford University School of Medicine, 265 Campus Drive, Room G1120B, Stanford, CA 94305, USA
[2]Department of Bioengineering, Stanford University Schools of Medicine and Engineering, Stanford, CA 94305, USA
[3]Institute for Stem Cell Biology and Regenerative Medicine, Stanford University School of Medicine, Stanford, CA 94305, USA
[4]Smidt Heart Institute, Cedars-Sinai Medical Center, Los Angeles, CA 90048, USA
[5]Board of Governors Regenerative Medicine Institute, Cedars-Sinai Medical Center, Los Angeles, CA 90048, USA
[6]BioServe Space Technologies, Department of Aerospace Engineering Sciences, University of Colorado, Boulder, CO 80309, USA
[7]Astronaut Office, NASA Johnson Space Center, Houston, TX 77058, USA
[8]Department of Medicine, Division of Cardiology, Stanford University School of Medicine, Stanford, CA 94305, USA
[9]Department of Surgery, The Ohio State University, Columbus, OH 43210, USA
[10]Department of Biomedical Engineering, The Ohio State University, Columbus, OH 43210, USA
[11]Co-first author
*Correspondence: joewu@stanford.edu
https://doi.org/10.1016/j.stemcr.2019.10.006

SUMMARY

With extended stays aboard the International Space Station (ISS) becoming commonplace, there is a need to better understand the effects of microgravity on cardiac function. We utilized human induced pluripotent stem cell-derived cardiomyocytes (hiPSC-CMs) to study the effects of microgravity on cell-level cardiac function and gene expression. The hiPSC-CMs were cultured aboard the ISS for 5.5 weeks and their gene expression, structure, and functions were compared with ground control hiPSC-CMs. Exposure to microgravity on the ISS caused alterations in hiPSC-CM calcium handling. RNA-sequencing analysis demonstrated that 2,635 genes were differentially expressed among flight, post-flight, and ground control samples, including genes involved in mitochondrial metabolism. This study represents the first use of hiPSC technology to model the effects of spaceflight on human cardiomyocyte structure and function.

INTRODUCTION

The allure of space as a natural laboratory stems from its unique properties that cannot be perfectly duplicated on Earth, notably microgravity, which has been simulated using techniques such as rotating bioreactors, random positioning machines, and magnetic levitation (Becker and Souza, 2013). While spaceflight is largely government funded, private enterprises dedicated to low-orbit payload delivery have enabled space to become a realistic destination for science (Rogers, 2001). However, the effects of microgravity on human organ function must be better understood. Because of the heart's critical role in maintaining proper bodily systemic functions, the effects of microgravity on cardiac physiology, metabolism, and cellular biology should be elucidated.

Spaceflight induces physiological changes in cardiac function (Sides et al., 2005). Astronauts on space shuttle missions experienced reduced heart rate and lowered arterial pressure (Fritsch-Yelle et al., 1996; Perhonen et al., 2001). The National Aeronautics and Space Administration (NASA) Twin Study demonstrated that long-term exposure to microgravity reduces mean arterial pressure and increases cardiac output (Garrett-Bakelman et al., 2019). However, little is known about the role of microgravity in influencing human cardiac function at the cellular level.

Existing cardiac cellular microgravity studies have used mouse or rat cardiomyocyte (CM) models. Alterations occur in mRNA expression of rat cardiac myosin protein, critical for CM contractility, when animals are maintained in microgravity (Thomason et al., 1992). Microgravity upregulates the expression of mitochondrial metabolism genes, such as malate dehydrogenase, in rat cardiac muscle (Connor and Hood, 1998). Hindlimb suspension of rats promoted the expression of a unique isoform of cardiac troponin I, critical for proper CM contraction (Yu et al., 2001). In rat CMs, simulated microgravity altered nuclear localization of nuclear factor κB, which is implicated in the cellular response to oxidative stress (Kwon et al., 2009). However, animal models cannot perfectly replicate cellular functions in human cardiac tissues, partly due to species-specific differences in cardiac function (Fermini et al., 1992; Gauthier et al., 1999; Spotnitz et al., 1984). Thus, we should understand the cellular and physiological processes influenced by microgravity in human heart cells.

Human CMs are a limited resource and cannot be maintained long term (Bergmann et al., 2009). However,

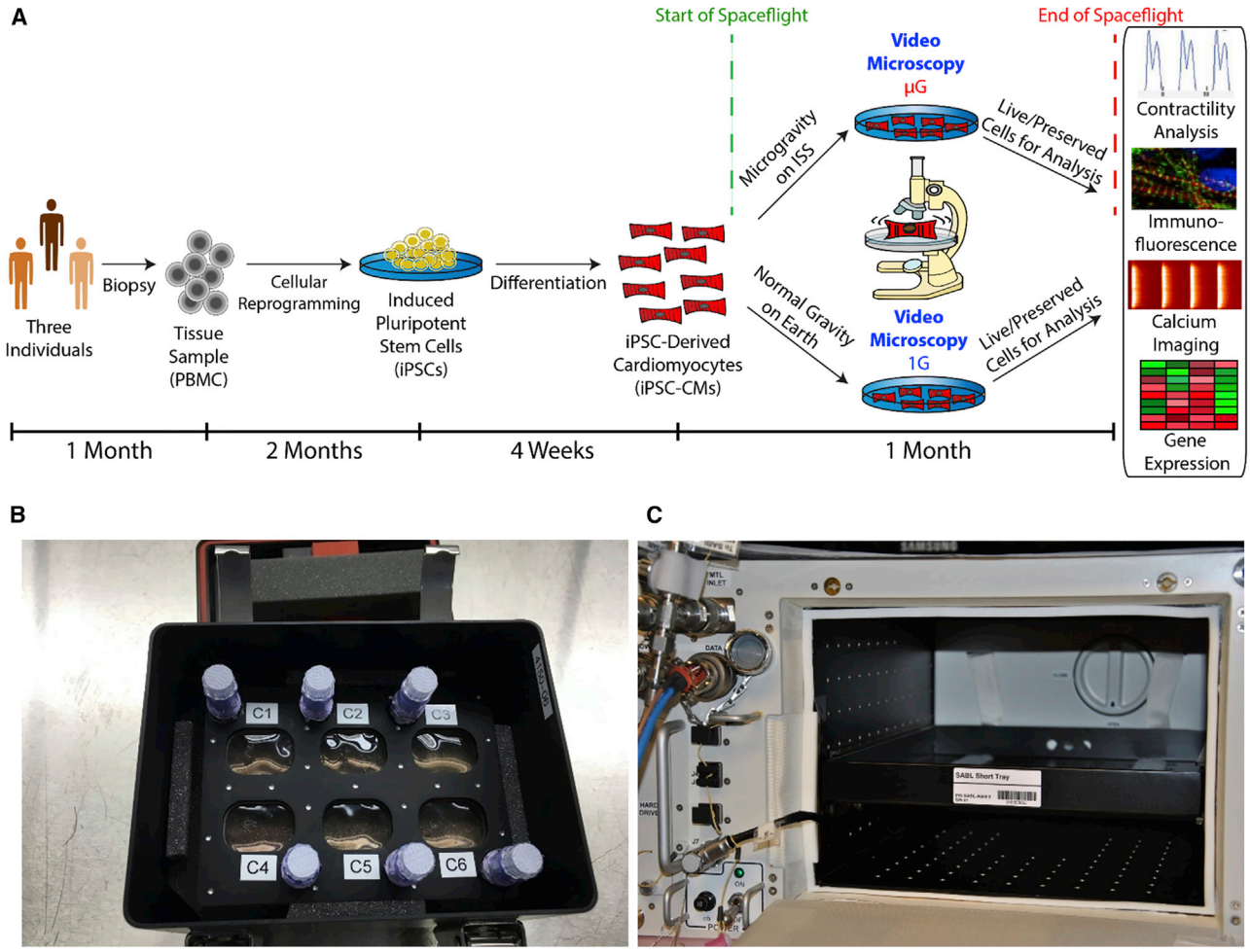

Figure 1. Evaluating the Effects of Spaceflight on hiPSC-CM Structure and Function

(A) Timeline for experiment. Tissue samples were collected from three individuals and used to generate human induced pluripotent stem cell-derived cardiomyocytes (hiPSC-CMs). The hiPSC-CMs were plated in fully enclosed 6-well plates optimized for microgravity ("BioCells") and sent to the International Space Station (ISS) for culture and live imaging for ~1 month. Ground controls with the same hiPSC-CM lines and hardware were maintained at Stanford University. Media exchanges and imaging were strictly scheduled so that the only significant difference in cell environment was spaceflight. After sample return from the ISS, cellular phenotypes were evaluated using gene expression, immunofluorescence, calcium imaging, and contractility analyses.

(B) A BioCell in its environmental control habitat ("PHAB").

(C) The interior of the Space Automated Bioproduct Laboratory (SABL), the incubator used to maintain the cells on the ISS.

human induced pluripotent stem cell-derived CMs (hiPSC-CMs) have emerged as a surrogate for studying the molecular and cellular mechanisms of human cardiac pathophysiology (Sharma et al., 2013, 2017, 2018; Sun et al., 2012). The hiPSC-CMs can be mass produced, cultured long term, and manipulated *in vitro* (Sharma et al., 2013). Employing a multi-disciplinary approach and access to the International Space Station (ISS), we utilized hiPSC-CMs to provide insights into the effects of spaceflight and microgravity on human cardiac physiology, cell structure, and gene expression.

RESULTS

Microgravity Cell Culture and Maintenance of hiPSC-CMs in Space

hiPSC lines were generated from three individuals by reprogramming peripheral blood mononuclear cells (PBMCs) and differentiating them into hiPSC-CMs (Burridge et al., 2014). Monolayers of beating hiPSC-CMs were sent to the ISS for 5.5 weeks (Figure 1A). The hiPSC-CMs were grown in fully enclosed 6-well plates (BioCells) optimized for long-term microgravity cell culture

(Figure 1B). BioCells were launched to the ISS aboard a SpaceX Dragon transport spacecraft via a SpaceX Falcon 9 rocket during the SpaceX CRS-9 commercial resupply service mission. BioCells were maintained aboard the ISS in an on-station incubator (Space Automated Bioproduct Laboratory [SABL]) (Figure 1C) at 37°C and 5% CO_2, and ground control cells were cultured in parallel. The hiPSC-CMs within the BioCells were cultured in a high-nutrient CM maintenance medium that was changed weekly. Ground control hiPSC-CMs were maintained identically, with media changes replicated exactly on a 6-h delay from the ISS.

Functional Analyses of hiPSC-CMs in Microgravity Conditions and Post Spaceflight

Prolonged spaceflight alters human heart physiology. Thus, we aimed to determine the effects of microgravity on hiPSC-CM morphology and function. Upon return to Earth, space-flown hiPSC-CMs were evaluated for changes in morphology and structure. Phase-contrast microscopy found no overt changes between groundside controls and flight samples (Figure 2A). The hiPSC-CMs from cell line 2 exhibited lower cell confluence than other lines, likely due to lower survival at initial plating. Immunofluorescence of ground and flight samples for sarcomeric proteins α-actinin and cardiac troponin T (cTnT) illustrated standard, striated sarcomeres (Figure 2B). DAPI-positive and cTnT/α-actinin-negative cells indicated the presence of a non-myocyte, fibroblast-like population. We did not observe significant differences in sarcomere structure, length, or regularity between ground and flight samples (Figures 2C–2E). These results suggest that space-flown hiPSC-CMs retain sarcomeric structure and morphology when compared with ground hiPSC-CMs.

For hiPSC-CM functional assessment, we analyzed hiPSC-CM contractile properties using video microscopy (Videos S1 and S2) with motion vector analysis (Huebsch et al., 2015). Ground and space-flown hiPSC-CMs had a similar spontaneous beat rate after 2.5 weeks (Figure 3A). There was no significant difference between contraction and relaxation velocities (Figures 3B and 3C). We also assessed Ca^{2+}-handling properties of space-flown hiPSC-CMs after return to Earth (Figure 3D). Space-flown hiPSC-CMs exhibited unchanged Ca^{2+} transient amplitude but showed a significant increase in transient decay tau (Figures 3E and S1) that is indicative of a decreased calcium recycling rate. We also observed an increase in the standard deviation of beating intervals (Figure 3F) in space-flown hiPSC-CMs, indicating beating irregularity. These results suggest that calcium-handling-related parameters remain altered for space-flown hiPSC-CMs following return to normal gravity.

Gene Expression of hiPSC-CMs in Microgravity and Post Spaceflight

We analyzed the transcriptome of hiPSC-CMs during spaceflight and post-flight. hiPSC-CMs were harvested at 4.5 weeks in spaceflight and on day 10 after return to Earth. Ground hiPSC-CMs were collected at the post-return time point as controls. Based on RNA sequencing, principal component analyses of flight, post-flight, and ground hiPSC-CMs showed that samples clustered based on the cell line of origin (Figure S2A) and developed a differential pattern of gene expression during the experiment. Flight samples clustered separately from post-flight samples, which in turn clustered most closely with ground controls (Figure 4A).

Based on our contractility and calcium-handling data, we examined expression of genes related to these functions. There was no significant change in expression levels of calcium cycling-related genes ryanodine receptor 2 (*RYR2*) or sarcoplasmic/ER calcium ATPase 2 (*SERCA2*) (Figure 4B). Thus, the declined calcium recycling we observed may have resulted from stress-induced calcium sarcoplasmic reticulum (SR) load increase, shifting the calcium balance between the SR and cytoplasm and decreasing the recycling rate through the same amount of SERCA2a. Increased SR load may increase calcium leak from RyR2, which would promote the beating irregularity we observed.

Sarcomeric genes cardiac troponin T (*TNNT2*) and troponin I1 (*TNNI1*) were significantly upregulated in flight, although other sarcomeric genes were similarly expressed (*MYH7*). Motif enrichment analysis of differentially expressed genes among the conditions (Table S2) indicated that the motif for specificity protein 1 (*Sp1*) was enriched for genes upregulated in flight compared with ground. *Sp1* activates the *TNNT2* promoter, which can contribute to a hypertrophic phenotype (Azakie et al., 2006).

Myocyte enhancer factor 2 (MEF2) transcription factor motifs were enriched in genes upregulated in flight compared with ground. Like *Sp1*, MEF2 contributes to regulation of a hypertrophic phenotype (Agrawal et al., 2010). *MEF2D*, which mediates stress-dependent cardiac remodeling (Kim et al., 2008), was upregulated in flight hiPSC-CMs compared with that on the ground (Figure 4C). Association of MEF2 with class II histone deacetylases (HDACs) represses hypertrophy, whereas class I HDACs induce hypertrophy (Agrawal et al., 2010). Expression of *HDAC10* and *HDAC4* (class II) was lower in flight hiPSC-CMs than on the ground, whereas expression of *HDAC8* (class I) was increased.

Other transcription factors for which motifs were enriched include peroxisome proliferator-activated receptors, Krüppel-like factor 5 (*KLF5*), and chicken ovalbumin upstream promoter transcription factor II (*COUP-TFII*), which

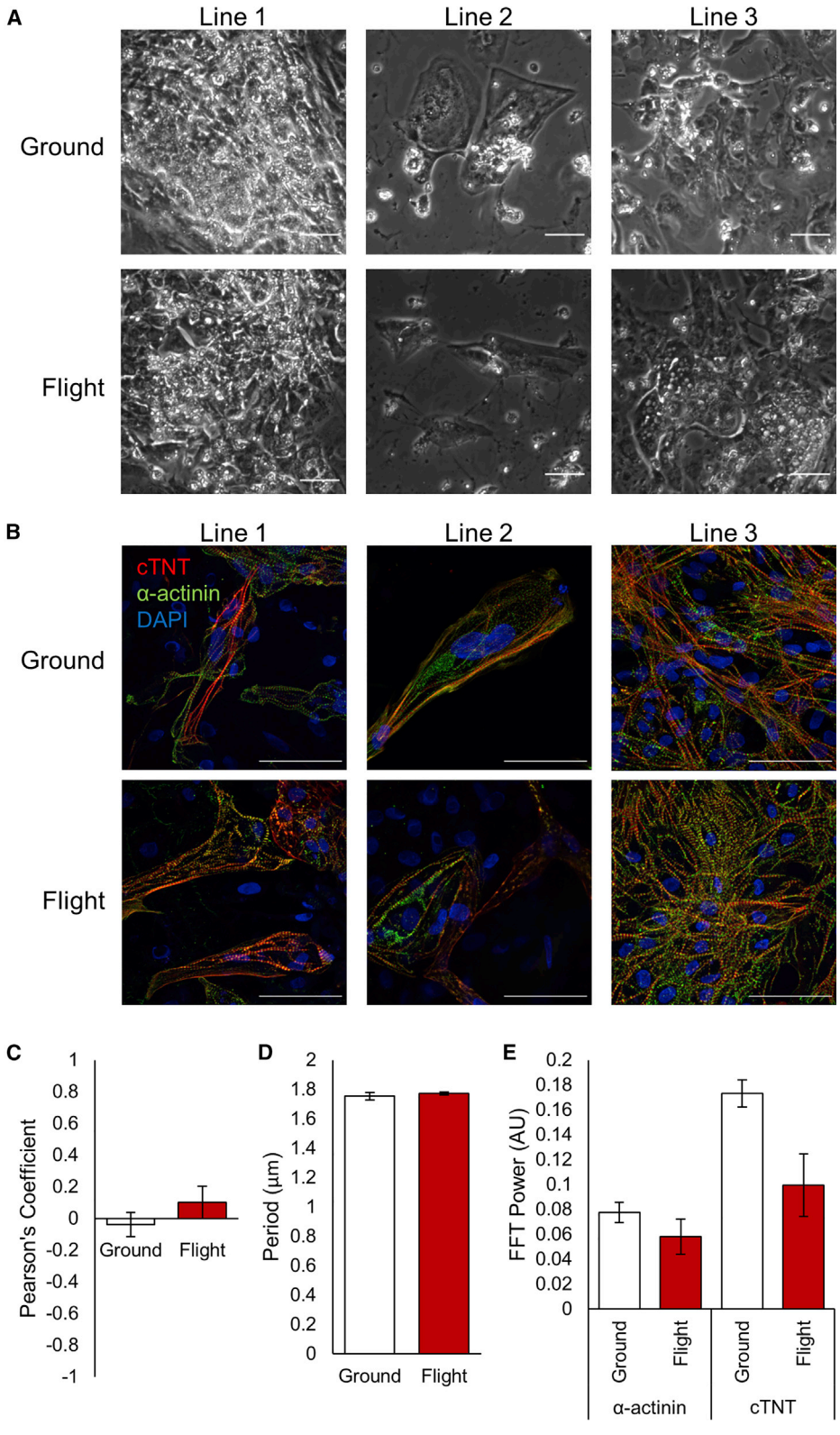

(legend on next page)

are involved in regulating cardiac metabolism (Drosatos et al., 2016; Wu et al., 2015). Although expression of these factors was not significantly different among the three conditions (Figure 4D), further annotation of RNA-sequencing data revealed that genes belonging to the mitochondrial metabolic pathway showed the most significant changes both between flight and ground and between flight and post-flight (Figures 4E and S2B; Table S3). Flight samples showed a decreased expression of genes related to RNA/DNA helicase and DNA damage and repair compared with both post-flight and ground samples. The numbers of differentially expressed genes in a two-group comparison between ground and flight (3,008 genes) and between post-flight and flight (2,026 genes) were much greater than the number of differentially expressed genes between post-flight and ground (1,049 genes), with the most overlap in differentially expressed genes between the ground versus flight and post-flight versus flight comparisons (Figure 4F). These results suggest that hiPSC-CMs adopt a unique gene-expression signature during spaceflight, and this gene-expression pattern reverts to one similar to ground controls upon return to normal gravity.

DISCUSSION

Decades of observations on space-flown animal models and human astronauts have confirmed that cardiovascular physiology is profoundly changed by spaceflight (Hughson et al., 2017). However, most cardiovascular microgravity physiology studies have been conducted either in non-human models or at tissue, organ, or systemic levels. While recent studies of human cardiac progenitor cells have demonstrated that microgravity can enhance their differentiation and maintenance (Baio et al., 2018; Camberos et al., 2019; Jha et al., 2016), none have addressed the effects of spaceflight on differentiated cardiomyocytes. Using 6-well plates optimized for microgravity, we sent live hiPSC-CMs from three individuals to the ISS as an *in vitro* human model for microgravity exposure.

Previous microgravity studies in animal models have demonstrated changes in contractile muscle protein expression (Thomason et al., 1992; Yu et al., 2001). While we did not observe a significant difference in contractility or differences in cell morphology or sarcomere structure between space-flown and groundside CMs, we did observe changes in calcium recycling and expression of myofilament genes in space-flown hiPSC-CMs. These findings parallel the aforementioned organ-level observations and suggest that, even at the cellular level, human CMs can functionally respond to changes in apparent gravity.

Gene-expression pathways related to mitochondrial function were upregulated in space-flown hiPSC-CMs. Binding motifs for transcription factors known to regulate cardiac metabolism were enriched in space-flown hiPSC-CMs. These results align with previous studies showing that the rat heart undergoes mitochondrial adaptations via gene upregulation after short-term exposure to microgravity (Connor and Hood, 1998). The NASA Twin Study also noted mitochondrial-related gene-expression changes (Garrett-Bakelman et al., 2019). Although their analysis was performed in PBMCs, the presence of mitochondrial gene-expression changes in their study and ours indicates that a cellular-level response to spaceflight may not be cell-type specific. Annotation of genes upregulated in post-flight compared with ground indicated that mitochondrial pathways were still enriched, demonstrating that a return to normal gravity does not completely restore normal mitochondrial gene expression, at least not within the first 10 days after return. Motif enrichment analysis also demonstrated that motifs enriched in genes upregulated in space-flown hiPSC-CMs were associated with transcription factors known to regulate hypertrophic pathways.

While we identified mitochondria- and hypertrophy-related pathways as those of interest, our conclusions are limited by time scale and available methods for this study. Longer exposure to microgravity or a longer readjustment period to normal gravity may change the extent of irreversible and reversed gene-expression changes, respectively. Additionally, the flight RNA samples were preserved at a different time points than the post-flight and ground samples, which may have contributed to the observed differences in gene expression. Finally, while we matched media change timing and environmental conditions for ground and flight samples as closely as possible, we note additional variables. For example, radiation levels are higher aboard the ISS than on Earth. Also, flight samples experienced launch and re-entry, whereas ground samples did not.

Figure 2. hiPSC-CMs Demonstrate No Overt Changes in Cell Morphology or Sarcomere Structure after Return from Spaceflight

(A) Representative phase-contrast images of live-return hiPSC-CMs from each cell line 3 days after sample return from the ISS, prior to paraformaldehyde fixation.

(B) Immunofluorescence of flight and ground control samples from each cell line showing sarcomeric proteins cardiac troponin T (cTnT) and α-actinin, and nuclear stain DAPI. Scale bars represent 50 μm.

(C–E) Pearson's coefficient (C), period (D), and fast Fourier transform (E) power of cTnT and α-actinin signals along sarcomere lines for ground and flight samples (arbitrary units). N = 3 lines, n = 2–3 images per line, with 8–15 sarcomeres analyzed per image.

Error bars represent standard error of the mean (SEM).

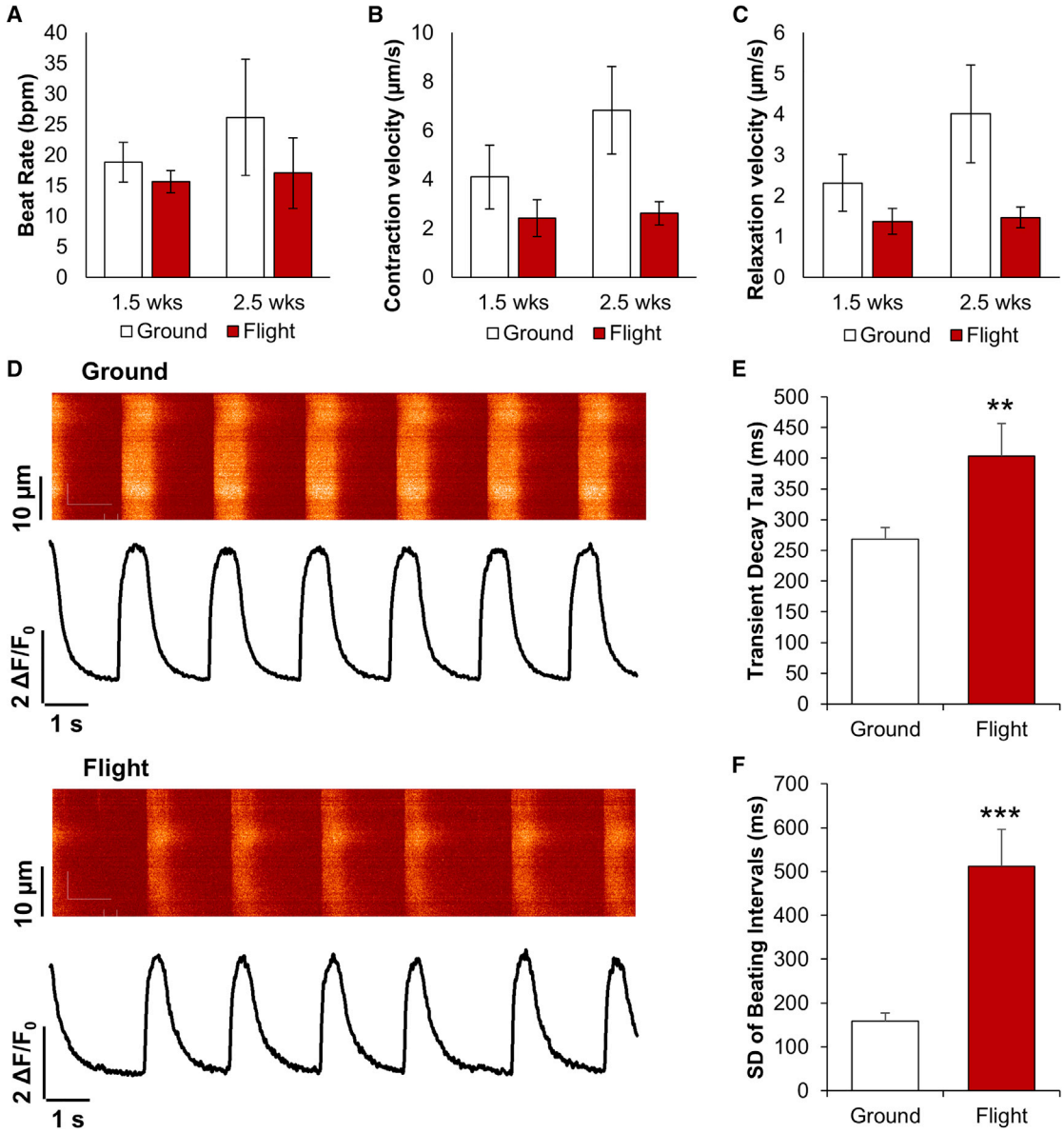

Figure 3. hiPSC-CM Contraction and Calcium Handling Are Altered by Spaceflight

(A–C) Beat rate in beats per minute (bpm) (A), contraction velocity (B), and relaxation velocity (C) for ground control and flight hiPSC-CMs after 1.5 and 2.5 weeks of culture on the ISS. N = 3 lines, n = 1–2 biological replicates per line, with 1–4 videos per sample.

(D) Representative calcium transients for ground and flight conditions, measured 3 days after live return from the ISS.

(E and F) Transient decay tau (E) and standard deviation of beating intervals (F) from calcium transients. N = 103 and 34 cells in ground and flight groups, respectively. **$p < 0.01$ and ***$p < 0.001$ versus ground control.

Error bars represent SEM. See also Figure S1; Videos S1 and S2.

The forces that cells experienced during transit may have affected their phenotype and gene expression. In future studies, including a 1G centrifuge control on the ISS or a simulated microgravity control on the ground may help disaggregate these effects.

There are also well-established caveats to using hiPSC-CMs. We noted the presence of non-cardiomyocyte, fibroblast-like cells in each hiPSC-CM line, likely due to incomplete metabolic selection of hiPSC-CMs prior to spaceflight. Perfect purification of hiPSC-CMs remains an issue during differentiation, and long-term metabolic selection using a low-glucose medium is often unable to completely eliminate fibroblasts. Residual fibroblasts may have proliferated during this month-long experiment.

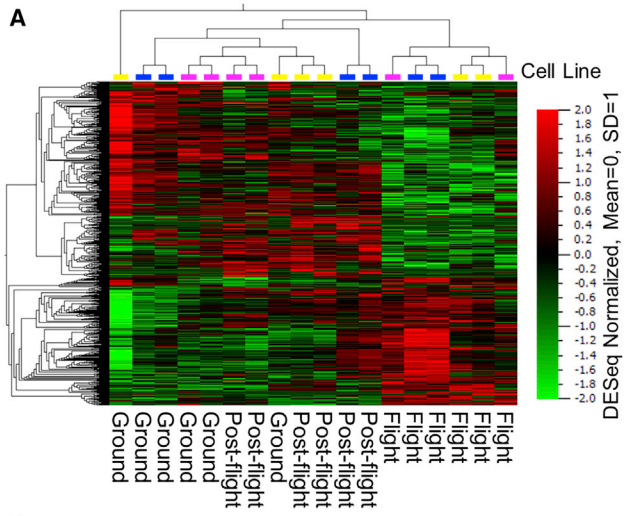

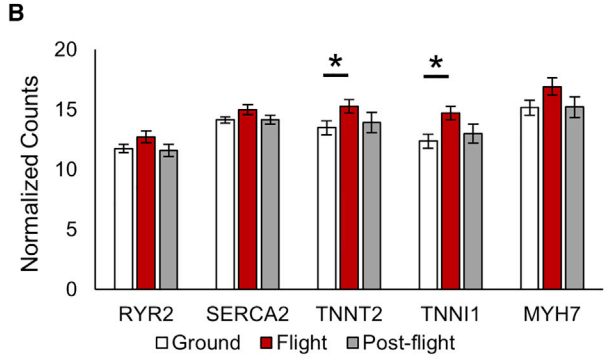

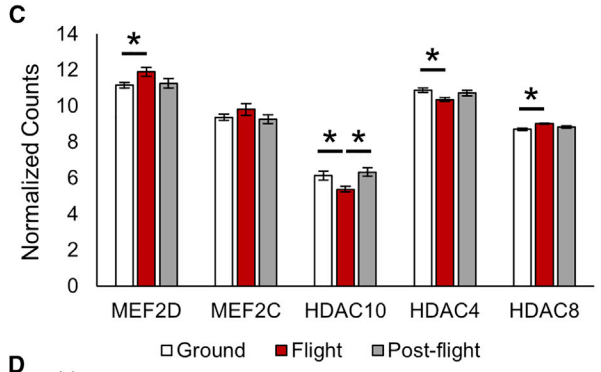

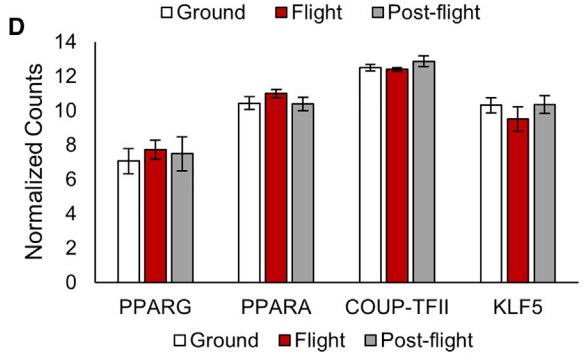

E

(A) Down in post-flight vs. ground **(D)** Up in post-flight vs. ground
(B) Down in flight vs. post-flight **(E)** Up in flight vs. post-flight
(C) Down in flight vs. ground **(F)** Up in flight vs. ground

	A	B	C	D	E	F
Helicase	0.29	4.97	2.65			
Iron-sulfur binding						2.23
DNA damage and repair		3.49	2.18	0.36	0.1	0.11
BTB domain	1.02	0.46	4.56		0.05	
Zinc finger region			2.06			
Zinc finger region, transcription regulation	4.75	0.87	7.82	0.04	0.2	0.004
tRNA processing and modification		3.36				
Ribosome, mitochondrial translation				1.75	0.67	8.87
ATP and nucleotide binding		4.2	3.09			
NAD binding			0.28		0.43	2.66
Mitochondrial transolcation						2.11
Aerobic respiration, mitochondrial respiratory chain						4.29
Mitochondrion, transit peptide				6.69	2.38	48.87
Electron transport, mitochondrial respiratory chain					1.18	14.7
Cardiac muscle contraction, mitochondrial respiration						6.17
Oxidation-reduction, oxidoreductase		0.57	0.22		1.69	6.99
Dehydrogenase/reductase					0.45	3.41
Aldo/keto reductase					1.63	2.34
Lipid metabolism						2.36
Peroxisome						2.18
Ubiquitin-mediated proteolysis					2.12	
Protein Ubiquination					4.37	1.98
Ubiquitin-conjugating enzyme					2.17	2.23
Cilium morphogenesis, biogenesis, and assembly	0.45	0.78	3.4			
Primary cilium			2.03			

F

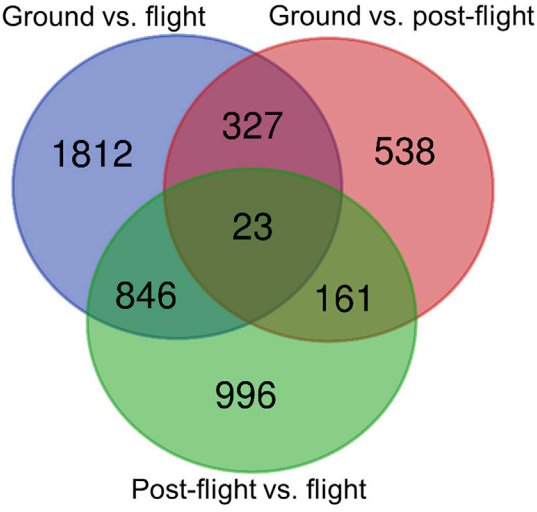

(legend on next page)

Additionally, hiPSC-CMs typically exhibit an immature human cardiac phenotype that is reflected in the contractility, force output, electrophysiology, and overall structure of these cells, all of which differ from true adult human CMs (Oikonomopoulos et al., 2018). However, we still believe that hiPSC-CMs represent the best model currently available for studying cell-level human cardiac function in response to environmental stimuli such as microgravity.

Further investigations into cardiac response to spaceflight are necessary to confirm these results and elucidate the mechanism of response to microgravity. Studies of functional changes in mitochondria of CMs exposed to microgravity would complement the gene-expression changes we observed. Using three-dimensional, tissue-like structures, such as engineered heart tissues or cardiac organoids, would provide a more physiologically accurate model and allow study of interactions between multiple cell types (Wnorowski et al., 2019). Eventually, these platforms may enable prevention or treatment strategies to be developed for spaceflight-induced cardiac remodeling.

Our study demonstrated for the first time that hiPSC-CMs can model the effects of spaceflight and microgravity. Human heart muscle cells, like the whole heart, change their functional properties in spaceflight and compensate for the apparent loss of gravity by altering their gene-expression patterns at the cellular level. As humans spend more time in space, we must better understand the effects of spaceflight on human physiology at the cellular level. Here, we demonstrated that long-term cell culture of advanced, highly specialized cell types such as human CMs is possible aboard the ISS and that such studies can provide informative data. We also laid the groundwork for future studies that will employ next-generation technologies, such as three-dimensional organoids, organ or body-on-a-chip systems, and high-throughput screening platforms, to more accurately model cardiac and human physiology in spaceflight.

EXPERIMENTAL PROCEDURES

Full details are provided in Supplemental Experimental Procedures.

hiPSC-CM Differentiation and Culture

All hiPSCs were derived with approval from the Institutional Review Board at Stanford University. hiPSCs were cultured on Matrigel-coated plates and differentiated into hiPSC-CMs using two-dimensional monolayer differentiation (Burridge et al., 2014).

Custom Spaceflight Hardware (BioServe Space Technologies)

Plate Habitat

The Plate Habitat (PHAB) is an aluminum box that can be sealed or vented. When transporting live mammalian cells to the ISS, the PHAB is charged with 5% CO_2. Vents are then sealed with a cover made of aluminum and Kapton tape. The PHAB, in this configuration, can maintain 4.5%–5% CO_2 for up to 9 days once charged and sealed. On board the ISS, the vent cover is removed and the PHAB is placed in an on-board incubator (SABL) that provides 37°C and active 5% CO_2 control. The PHAB provides containment for liquids as per NASA safety protocol.

BioCell

The BioCell is a fully contained cell culture vessel for ISS use. The 6-well BioCell has an aluminum frame and a polysulfone center with 6 individual wells, each with its own access port. A gas-permeable membrane covers both sides of the well. The membrane also provides the growth surface for cells being cultured within each well. Each well has a maximum volume of 2.5 mL. Fluid exchanges are completed by attaching a syringe to each access port and then exchanging the fluid in the well with the fluid in the syringe.

Space Automated Bioproduct Laboratory

The SABL is a "smart" incubator currently aboard the ISS that can hold temperatures between −5°C and 43°C. For mammalian cell culture, BioServe's Atmosphere Control Module (ACM) is inserted into SABL and provides 5% CO_2. For this hiPSC-CM experiment, the SABL with ACM installed was used to house three PHABs, each with a 6-well BioCell. Temperature set points for SABL are controlled from the ground via BioServe's Payload Operations and Command Center.

ACCESSION NUMBERS

RNA-sequencing data for this article are available on the Gene Expression Omnibus with accession number GEO: GSE137081.

SUPPLEMENTAL INFORMATION

Supplemental Information can be found online at https://doi.org/10.1016/j.stemcr.2019.10.006.

Figure 4. hiPSC-CM RNA Expression Profiles Are Altered by Spaceflight

RNA-sequencing data comparing flight samples preserved in RNAlater after ~4.5 weeks in microgravity, post-flight samples preserved 10 days post return after ~5.5 weeks in microgravity, and ground control samples preserved at the same time as post-flight samples.

(A) Heatmap displaying 2,635 genes differentially expressed among the three groups with $p \leq 0.05$.

(B–D) Expression of genes related to (B) calcium handling and contraction, (C) hypertrophy, and (D) metabolism, with *$p \leq 0.05$.

(E) Group enrichment scores for top functional annotation clusters (enrichment score ≥ 2 for at least one group) determined using the Database for Annotation, Visualization, and Integrated Discovery (DAVID) for genes differentially expressed between the indicated groups with $p \leq 0.05$ based on a two-tailed Student's t test.

(F) Venn diagram demonstrating differentially expressed genes for each comparison with $p \leq 0.05$ based on a two-tailed Student's t test.

See also Figure S2 and Tables S1, S2, and S3.

AUTHOR CONTRIBUTIONS

A.W. and A.S.: conception and design, data collection, data analysis, and manuscript writing; H.C., H.W., N.-Y.S., and C.L.: data collection and data analysis; N.S.: data collection, data analysis, and manuscript writing; K.H.R.: conception, design, and data collection; S.C. and L.S.S.: conception and design; S.M.W. and P.H.U.L.: conception, design, and manuscript writing; J.C.W.: conception and design, financial support, manuscript writing, and final approval of manuscript.

ACKNOWLEDGMENTS

We gratefully acknowledge support from Department of Defense National Defense Science and Engineering Graduate Fellowship (A.W.), American Heart Association (AHA) Predoctoral Fellowship 13PRE15770000, National Science Foundation (NSF) Graduate Research Fellowship Program DGE-114747, NIH T32 HL116273 (A.S.), NIH K99 HL133473, AHA postdoctoral fellowship (16POST31150011) (H.W.), NIH K01 HL135455 (N.S.), NIH Director's Pioneer Award (DP1 LM012179-02), NHLBI Progenitor Cell Biology Consortium (U01 HL099776), AHA Grant-in-Aid (14GRNT18630016) (S.M.W.), Burroughs Wellcome Foundation Innovation in Regulatory Science 1015009, AHA 17MERIT33610009, Center for the Advancement of Science in Space (CASIS) GA-2014-129, NIH R01 HL141371, and NIH UG3 TR002588 (J.C.W.). We also acknowledge the Stanford Neuroscience Microscopy Service (NIH NS069375). We thank our implementation partners at BioServe Space Technologies and SpaceX. Finally, we thank the students and teachers of the Orion's Quest educational program for their assistance with data analysis and encourage them to continue pursuing their passion for science. J.C.W. is a co-founder of Khloris Biosciences but has no competing interests, as the work presented here is completely independent. The other authors declare no competing interests.

Received: April 24, 2019
Revised: October 9, 2019
Accepted: October 10, 2019
Published: November 7, 2019

REFERENCES

Agrawal, R., Agrawal, N., Koyani, C.N., and Singh, R. (2010). Molecular targets and regulators of cardiac hypertrophy. Pharmacol. Res. *61*, 269–280.

Azakie, A., Fineman, J.R., and He, Y. (2006). Sp3 inhibits Sp1-mediated activation of the cardiac troponin T promoter and is downregulated during pathological cardiac hypertrophy in vivo. Am. J. Physiol. Circ. Physiol. *291*, H600–H611.

Baio, J., Martinez, A.F., Silva, I., Hoehn, C.V., Countryman, S., Bailey, L., Hasaniya, N., Pecaut, M.J., and Kearns-Jonker, M. (2018). Cardiovascular progenitor cells cultured aboard the International Space Station exhibit altered developmental and functional properties. NPJ Microgravity *4*, 13.

Becker, J.L., and Souza, G.R. (2013). Using space-based investigations to inform cancer research on Earth. Nat. Rev. Cancer *13*, 315–327.

Bergmann, O., Bhardwaj, R.D., Bernard, S., Zdunek, S., Barnabé-Heider, F., Walsh, S., Zupicich, J., Alkass, K., Buchholz, B.A., Druid, H., et al. (2009). Evidence for cardiomyocyte renewal in humans. Science *324*, 98–102.

Burridge, P.W., Matsa, E., Shukla, P., Lin, Z.C., Churko, J.M., Ebert, A.D., Lan, F., Diecke, S., Huber, B., Mordwinkin, N.M., et al. (2014). Chemically defined generation of human cardiomyocytes. Nat. Methods *11*, 855–860.

Camberos, V., Baio, J., Bailey, L., Hasaniya, N., Lopez, L.V., and Kearns-Jonker, M. (2019). Effects of spaceflight and simulated microgravity on YAP1 expression in cardiovascular progenitors: implications for cell-based repair. Int. J. Mol. Sci. *20*, 2742.

Connor, M.K., and Hood, D.A. (1998). Effect of microgravity on the expression of mitochondrial enzymes in rat cardiac and skeletal muscles. J. Appl. Physiol. *84*, 593–598.

Drosatos, K., Pollak, N.M., Pol, C.J., Ntziachristos, P., Willecke, F., Valenti, M.-C., Trent, C.M., Hu, Y., Guo, S., Aifantis, I., et al. (2016). Cardiac myocyte KLF5 regulates Ppara expression and cardiac function. Circ. Res. *118*, 241–253.

Fermini, B., Wang, Z., Duan, D., and Nattel, S. (1992). Differences in rate dependence of transient outward current in rabbit and human atrium. Am. J. Physiol. *263*, H1747–H1754.

Fritsch-Yelle, J.M., Charles, J.B., Jones, M.M., and Wood, M.L. (1996). Microgravity decreases heart rate and arterial pressure in humans. J. Appl. Physiol. *80*, 910–914.

Garrett-Bakelman, F.E., Darshi, M., Green, S.J., Gur, R.C., Lin, L., Macias, B.R., McKenna, M.J., Meydan, C., Mishra, T., Nasrini, J., et al. (2019). The NASA Twins Study: a multidimensional analysis of a year-long human spaceflight. Science *364*. https://doi.org/10.1126/science.aau8650.

Gauthier, C., Tavernier, G., Trochu, J.N., Leblais, V., Laurent, K., Langin, D., Escande, D., and Le Marec, H. (1999). Interspecies differences in the cardiac negative inotropic effects of β3-adrenoceptor agonists. J. Pharmacol. Exp. Ther. *290*, 687–693.

Huebsch, N., Loskill, P., Mandegar, M.A., Marks, N.C., Sheehan, A.S., Ma, Z., Mathur, A., Nguyen, T.N., Yoo, J.C., Judge, L.M., et al. (2015). Automated video-based analysis of contractility and calcium flux in human-induced pluripotent stem cell-derived cardiomyocytes cultured over different spatial scales. Tissue Eng. Part C Methods *21*, 467–479.

Hughson, R.L., Helm, A., and Durante, M. (2017). Heart in space: effect of the extraterrestrial environment on the cardiovascular system. Nat. Rev. Cardiol. *15*, 167–180.

Jha, R., Wu, Q., Singh, M., Preininger, M.K., Han, P., Ding, G., Cho, H.C., Jo, H., Maher, K.O., Wagner, M.B., et al. (2016). Simulated microgravity and 3D culture enhance induction, viability, proliferation and differentiation of cardiac progenitors from human pluripotent stem cells. Sci. Rep. *6*, 30956.

Kim, Y., Phan, D., van Rooij, E., Wang, D., McAnally, J., Qi, X., Richardson, J.A., Hill, J.A., Bassel-Duby, R., and Olson, E.N. (2008). The MEF2D transcription factor mediates stress-dependent cardiac remodeling in mice. J. Clin. Invest. *118*, 124–132.

Kwon, O., Tranter, M., Jones, W.K., Sankovic, J.M., and Banerjee, R.K. (2009). Differential translocation of nuclear factor-kappaB in

a cardiac muscle cell line under gravitational changes. J. Biomech. Eng. *131*, 064503.

Oikonomopoulos, A., Kitani, T., and Wu, J.C. (2018). Pluripotent stem cell-derived cardiomyocytes as a platform for cell therapy applications: progress and hurdles for clinical translation. Mol. Ther. *26*, 1624–1634.

Perhonen, M.A., Franco, F., Lane, L.D., Buckey, J.C., Blomqvist, C.G., Zerwekh, J.E., Peshock, R.M., Weatherall, P.T., and Levine, B.D. (2001). Cardiac atrophy after bed rest and spaceflight. J. Appl. Physiol. *91*, 645–653.

Rogers, T.F. (2001). "Space tourism"—its importance, its history, and a recent extraordinary development. Acta Astronaut *49*, 537–549.

Sharma, A., Wu, J.C., and Wu, S.M. (2013). Induced pluripotent stem cell-derived cardiomyocytes for cardiovascular disease modeling and drug screening. Stem Cell Res. Ther. *4*, 150.

Sharma, A., Burridge, P.W., McKeithan, W.L., Serrano, R., Shukla, P., Sayed, N., Churko, J.M., Kitani, T., Wu, H., Holmström, A., et al. (2017). High-throughput screening of tyrosine kinase inhibitor cardiotoxicity with human induced pluripotent stem cells. Sci. Transl. Med. *9*, eaaf2584.

Sharma, A., Toepfer, C.N., Ward, T., Wasson, L., Agarwal, R., Conner, D.A., Hu, J.H., and Seidman, C.E. (2018). CRISPR/Cas9-mediated fluorescent tagging of endogenous proteins in human pluripotent stem cells. Curr. Protoc. Hum. Genet. *96*, 21.11.1–21.11.20.

Sides, M.B., Vernikos, J., Convertino, V.A., Stepanek, J., Tripp, L.D., Draeger, J., Hargens, A.R., Kourtidou-Papadeli, C., Pavy-LeTraon, A., Russomano, T., et al. (2005). The Bellagio report: cardiovascular risks of spaceflight: implications for the future of space travel. Aviat. Space Environ. Med. *76*, 877–895.

Spotnitz, W.D., Clark, M.B., Rosenblum, H.M., Lazar, H.L., Haasler, G.B., Collins, R.H., Spotnitz, A.J., Wong, C.Y., and Spotnitz, H.M. (1984). Effect of cardiopulmonary bypass and global ischemia on human and canine left ventricular mass: evidence for interspecies differences. Surgery *96*, 230–239.

Sun, N., Yazawa, M., Liu, J., Han, L., Sanchez-Freire, V., Abilez, O.J., Navarrete, E.G., Hu, S., Wang, L., Lee, A., et al. (2012). Patient-specific induced pluripotent stem cells as a model for familial dilated cardiomyopathy. Sci. Transl. Med. *4*, 130ra47.

Thomason, D.B., Morrison, P.R., Oganov, V., Ilyina-Kakueva, E., Booth, F.W., and Baldwin, K.M. (1992). Altered actin and myosin expression in muscle during exposure to microgravity. J. Appl. Physiol. *73*, S90–S93.

Wnorowski, A., Yang, H., and Wu, J.C. (2019). Progress, obstacles, and limitations in the use of stem cells in organ-on-a-chip models. Adv. Drug Deliv. Rev. *140*, 3–11.

Wu, S.-P., Kao, C.-Y., Wang, L., Creighton, C.J., Yang, J., Donti, T.R., Harmancey, R., Vasquez, H.G., Graham, B.H., Bellen, H.J., et al. (2015). Increased COUP-TFII expression in adult hearts induces mitochondrial dysfunction resulting in heart failure. Nat. Commun. *6*, 8245.

Yu, Z.-B., Zhang, L.-F., and Jin, J.-P. (2001). A proteolytic NH2-terminal truncation of cardiac troponin I that is up-regulated in simulated microgravity. J. Biol. Chem. *276*, 15753–15760.

Stem Cell Reports, Volume *13*

Supplemental Information

Effects of Spaceflight on Human Induced Pluripotent Stem Cell-Derived Cardiomyocyte Structure and Function

Alexa Wnorowski, Arun Sharma, Haodong Chen, Haodi Wu, Ning-Yi Shao, Nazish Sayed, Chun Liu, Stefanie Countryman, Louis S. Stodieck, Kathleen H. Rubins, Sean M. Wu, Peter H.U. Lee, and Joseph C. Wu

Inventory of Supplemental Information

Figure S1. Additional hiPSC-CM calcium handling parameters. Related to Figure 3. This figure presents additional calcium imaging data from the analysis shown in Figure 3.

Figure S2. hiPSC-CM gene expression. Related to Figure 4. This figure presents PCR validation and additional analysis of the RNA-sequencing data shown in Figure 4.

Table S1. Differentially Expressed Genes in Multi-Group Comparison. Related to Figure 4. This table contains the expression data for the differentially expressed genes in the heat map in Figure 4A.

Table S2. Motif Enrichment Analysis. Related to Figure 4. This table contains the complete data for motif enrichment analysis, which was used to identify the transcription factors presented in Figures 4C and 4D.

Table S3. DAVID Functional Annotation Clustering. Related to Figure 4. This table contains complete data for the functional annotation clustering represented in Figure 4E.

Video S1. Representative flight contractility at 1.5 weeks. Related to Figure 3. A representative video used for contractility analysis displayed in Figures 3A-C.

Video S2. Representative ground contractility at 1.5 weeks. Related to Figure 3. A representative video used for contractility analysis displayed in Figures 3A-C.

Supplemental Figures

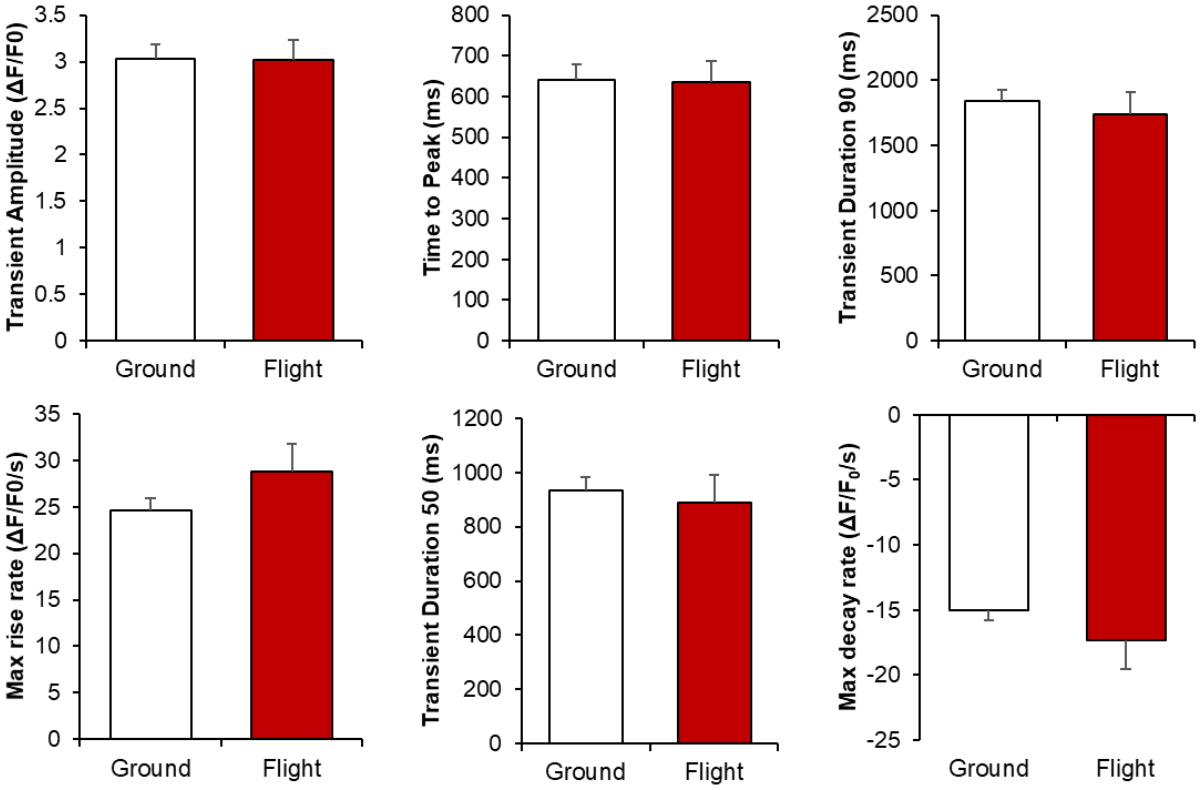

Figure S1. Additional hiPSC-CM calcium handling parameters. Related to Figure 3. Calcium transients were measured in flight and ground control hiPSC-CMs 3 days after live-return from the ISS and were used to calculate calcium handling parameters. N = 103 and 34 cells in ground and flight groups, respectively. Error bars represent standard error of the mean.

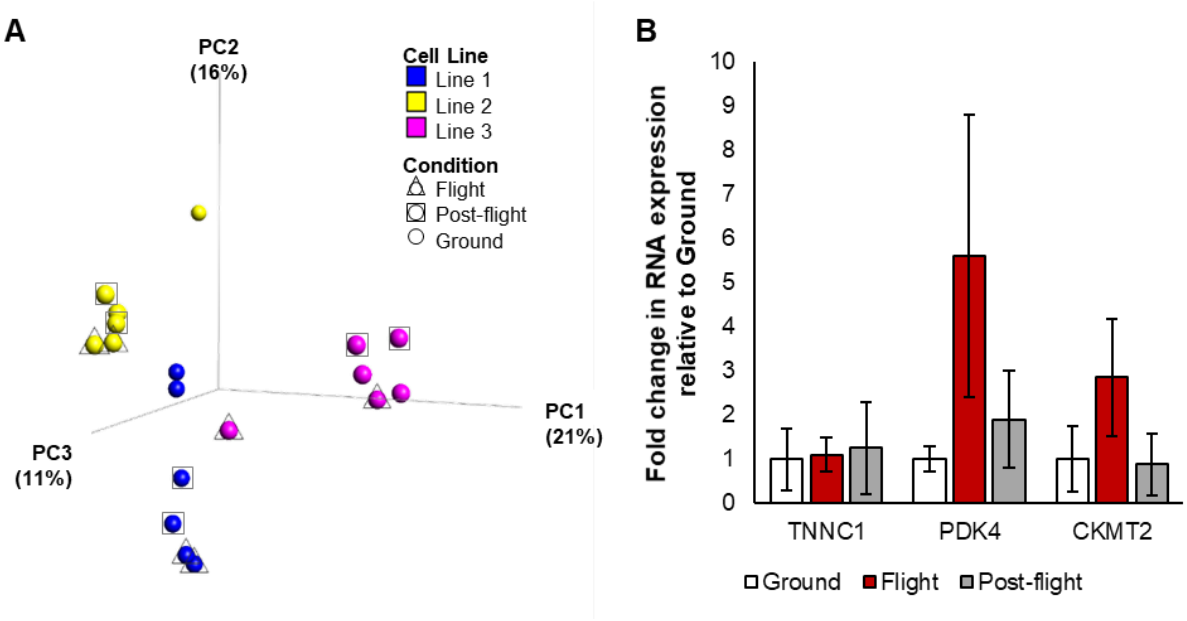

Figure S2. hiPSC-CM gene expression. Related to Figure 4. (A) PCA plot representing gene expression for each sample analyzed. Samples grouped more by cell line than by flight vs ground condition. **(B)** Fold-change in RNA expression of genes in "mitochondria, transit peptide" functional annotation category highlighted in Figure 4E as measured by quantitative PCR. Expression data were averaged by line and then by condition. Error bars represent standard error of the mean.

Supplemental Experimental Procedures

Differentiation of hiPSC-CMs. Three hiPSC lines were generated using a previously published Sendai virus reprogramming protocol on peripheral blood mononuclear cells from three healthy individuals (Churko et al., 2013). These hiPSC lines were differentiated into hiPSC-CMs using a 2D monolayer differentiation protocol and were maintained in a 5% CO_2/air environment as previously described (Lian et al., 2012; Sun et al., 2012). Briefly, hiPSC colonies were dissociated with 0.5 mM EDTA into single-cell suspension and resuspended in E8 media (Life Technologies) containing 10 μM Rho-associated protein kinase inhibitor (Sigma). Approximately 100,000 cells were replated into 6-well dishes pre-coated with Matrigel (BD Biosciences). Next, hiPSC monolayers were cultured to 85% cell confluency. Cells were then treated for 2 days with 6 μM CHIR99021 (Selleck Chemicals) in RPMI 1640+B27 supplement without insulin to activate Wnt signaling and induce mesodermal differentiation. On day 2, cells were placed in RPMI+B27 without insulin and without CHIR99021. On days 3-4, cells were treated with 5 μM IWR-1 (Sigma) to inhibit Wnt pathway signaling and induce cardiogenesis. On days 5-6, cells were removed from IWR-1 treatment and placed in RPMI+B27 without insulin. From day 7 onwards, cells were placed in RPMI+B27 with insulin until beating was observed. At this point, cells were glucose-starved for 3 days with RPMI (no glucose)+B27 with insulin to purify the hiPSC-CMs, as CMs can selectively metabolize fatty acids as an alternate source of cellular energy (Tohyama et al., 2013). Following purification, cells were cultured in RPMI 1640+B27 with insulin. When replating hiPSC-CMs for downstream use, cells were dissociated with 0.25% trypsin-EDTA (Life Technologies) into a single-cell suspension and seeded on Matrigel-coated "BioCell" 6-well plates customized for microgravity cell culture (BioServe Space Technologies).

Microgravity Cell Culture. hiPSC-CMs within the BioCells were cultured in a high-nutrient variant of cardiomyocyte maintenance media (RPMI 1640 with L-GlutaMAX + B27 with insulin + 15 mM Hepes + 5% PenStrep). Sterile syringes containing 10 mL of high nutrient culture media were attached to sterile ports on each well of the BioCell and pumped up and down 15 times to mix the fresh media with the spent media, producing an approximate 80% media change. Media changes for ground controls were completed in the same manner, with timing replicated exactly on a six-hour delay from the ISS.

Ca^{2+} Imaging. Three days after splash-down of flight samples from the ISS, hiPSC-CMs were treated with 5 μM Fluo-4 AM and 0.02% Pluronic F-127 (Molecular Probes) in Tyrode's solution for 15 minutes at 37°C. Cells were washed with Tyrode's solution afterward. Ca^{2+} imaging to examine calcium flux during hiPSC-CM contractility was conducted using a Zeiss LSM 510Meta confocal microscope (ZEISS) (20× Plan Apochromat NA 0.8). Spontaneous Ca^{2+} transients were obtained at 37°C using a single-cell line scanning mode (512 pixels*1920 lines). Ca^{2+} images were analyzed with a custom-made MATLAB algorithm.

Immunofluorescence and Microscopy. Immunostaining was performed according to previous protocols (Sharma et al., 2014). Briefly, membranes were cut out of the BioCell plates and placed in standard 6-well culture plates (Corning). Cells were fixed using 4% paraformaldehyde and treated with 0.1% TX-100 in PBS to permeabilize cell membranes. Primary antibodies for cardiac troponin T (Abcam AB45932) and cardiac alpha-actinin (Sigma A7811) were diluted 1:200 in 2% goat serum in PBS and incubated on the cells overnight. Secondary antibodies conjugated with fluorophores (Invitrogen A11029, A11037) were diluted 1:500 in 2% goat serum in PBS and incubated on the cells for 2 hours. Cell nuclei were stained using NucBlue™ Fixed Cell ReadyProbes™ Reagent (Invitrogen R37606) diluted in PBS for 20 minutes. Membranes were fixed to a coverslip using ProLong™ Gold Anti-Fade Reagent (Invitrogen P36931). Imaging was performed using a LSM710 confocal microscope (ZEISS) through the Stanford Neuroscience Microscopy Service facility.

Live Imaging and Contractility Assessment. Cells were imaged 9 and 16 days into space flight using a Nikon Eclipse TS100 microscope (ISS) and Leica DM IL LED microscope (ground). One plate from each group (flight vs ground) was used for imaging. Plates were removed from the incubator, imaged, and returned to the incubator on the same schedule, with the groundside control plate on a six-hour delay. Fifteen second videos were divided into regions of interest (ROI) containing one or more CM patches, with ROI size consistent within each video. ROIs were chosen to maximize covered beating cell area and minimize coverage of non-beating areas. ROI videos were converted to image sequences with a frame rate of 15 frames per second. Image sequences were analyzed using a MATLAB program described previously (Huebsch et al., 2016). Each contraction velocity trace was manually matched to the respective video and ROI to ensure the traces matched cardiomyocyte contraction.

RNA-sequencing Gene Expression Analysis. RNALater (Thermo Fisher) was used to preserve flight samples designated for downstream RNA-sequencing analysis. Samples preserved in RNALater were stored at 4°C until return to our laboratory, when RNA was isolated from preserved wells in the BioCells using RNeasy kit (Qiagen) following the manufacturer's protocol. DNase treatment was performed using RNase-free DNase kit (Qiagen). All RNA samples had RNA integrity number ≥ 8.9 and concentration ≥ 48 ng/µL (Agilent 2100 Bioanalyzer). Library prep and sequencing were performed by BGI with 30-40 million paired-end 100bp reads per sample on the Illumina HiSeq platform. The raw reads were aligned by HISAT2 (https://ccb.jhu.edu/software/hisat2/index.shtml)(Kim et al., 2015) to human genome (hg38). The aligned reads were quantitated by FeatureCounts (http://bioinf.wehi.edu.au/featureCounts/) with the annotation of ENSEMBL 85. The normalization and differentially expressed genes test were implemented by DESeq2 (https://bioconductor.org/packages/release/bioc/html/DESeq2.html) (Liao et al., 2014; Love et al., 2014). DESeq2 data were analyzed using Qlucore Omics Explorer Software. For the motif enrichment analysis, the promoter sequences of differentially expressed genes (upstream 400bp, downstream 100bp) were extracted from the human genome and fed to Hypergeometric Optimization of Motif EnRichment (HOMER) software (Heinz et al., 2010). The enriched motifs were then compared with the curated HOMER motif database. Database for Annotation, Visualization, and Integrated Discovery (DAVID) Bioinformatics Resources Functional Annotation Tool (version 6.8 - https://david.ncifcrf.gov/summary.jsp) was used to determine the functional annotation clusters of differentially expressed genes between each group, with differential gene lists based on a two-tailed Student's t-test with $p \leq 0.05$ (Huang et al., 2009a, 2009b). The Venn diagram of differentially expressed genes for each comparison was created using a tool through VIB/UGent Bioinformatics & Evolutionary Genomics (http://bioinformatics.psb.ugent.be/webtools/Venn/).

Statistical Methods. Data presented as mean ± SEM. Comparisons were conducted via Student's t-test with significant differences (*) defined by $p < 0.05$.

Supplemental References

Churko, J.M., Burridge, P.W., and Wu, J.C. (2013). Generation of human iPSCs from human peripheral blood mononuclear cells using non-integrative Sendai virus in chemically defined conditions. In Cellular Cardiomyoplasty: Methods in Molecular Biology (Methods and Protocols), pp. 81–88.

Heinz, S., Benner, C., Spann, N., Bertolino, E., Lin, Y.C., Laslo, P., Cheng, J.X., Murre, C., Singh, H., and Glass, C.K. (2010). Simple combinations of lineage-determining transcription factors prime cis-regulatory elements required for macrophage and B cell identities. Mol. Cell *38*, 576–589.

Huang, D.W., Sherman, B.T., and Lempicki, R.A. (2009a). Bioinformatics enrichment tools: paths toward the comprehensive functional analysis of large gene lists. Nucleic Acids Res. *37*, 1–13.

Huang, D.W., Sherman, B.T., and Lempicki, R.A. (2009b). Systematic and integrative analysis of large gene lists using DAVID bioinformatics resources. Nat. Protoc. *4*, 44–57.

Huebsch, N., Loskill, P., Deveshwar, N., Spencer, C.I., Judge, L.M., Mandegar, M.A., B. Fox, C., Mohamed, T.M.A., Ma, Z., Mathur, A., et al. (2016). Miniaturized iPS-cell-derived cardiac muscles for physiologically relevant drug response analyses. Sci. Rep. *6*, 24726.

Kim, D., Langmead, B., and Salzberg, S.L. (2015). HISAT: a fast spliced aligner with low memory requirements. Nat. Methods *12*, 357–360.

Lian, X., Hsiao, C., Wilson, G., Zhu, K., Hazeltine, L.B., Azarin, S.M., Raval, K.K., Zhang, J., Kamp, T.J., and Palecek, S.P. (2012). Robust cardiomyocyte differentiation from human pluripotent stem cells via temporal modulation of canonical Wnt signaling. Proc. Natl. Acad. Sci. *109*, E1848–E1857.

Liao, Y., Smyth, G.K., and Shi, W. (2014). featureCounts: an efficient general purpose program for assigning sequence reads to genomic features. Bioinformatics *30*, 923–930.

Love, M.I., Huber, W., and Anders, S. (2014). Moderated estimation of fold change and dispersion for RNA-seq data with DESeq2. Genome Biol. *15*, 550.

Sharma, A., Marceau, C., Hamaguchi, R., Burridge, P.W., Rajarajan, K., Churko, J.M., Wu, H., Sallam, K.I., Matsa, E., Sturzu, A.C., et al. (2014). Human induced pluripotent stem cell-derived cardiomyocytes as an in vitro model for coxsackievirus B3-induced myocarditis and antiviral drug screening platform. Circ. Res. *115*, 556–566.

Tohyama, S., Hattori, F., Sano, M., Hishiki, T., Nagahata, Y., Matsuura, T., Hashimoto, H., Suzuki, T., Yamashita, H., Satoh, Y., et al. (2013). Distinct metabolic flow enables large-scale purification of mouse and human pluripotent stem cell-derived cardiomyocytes. Cell Stem Cell *12*, 127–137.